 Development (2014) doi:10.1242/dev.103168

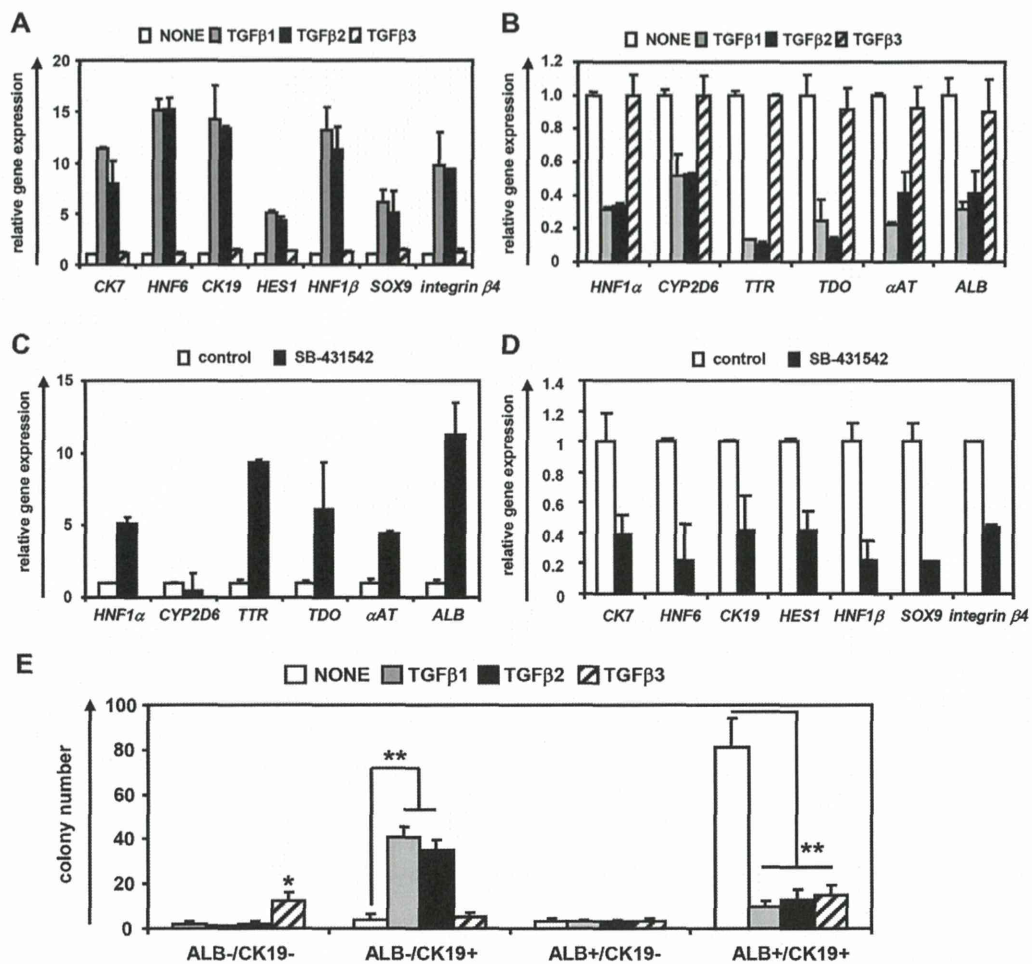

Fig. 2. Hepatocyte and cholangiocyte differentiation from HBCs is regulated by TGFβ signaling. (A,B) HBCs were cultured in differentiation hESF-DIF medium containing 10 ng/ml TGFβ1, TGFβ2 or TGFβ3 for 10 days. The expression levels of cholangiocyte (A) and hepatocyte (B) marker genes were measured by real-time RT-PCR. On the *y*-axis, the gene expression level of cholangiocyte markers in untreated cells (NONE) was taken as 1.0. (C,D) HBCs were cultured in differentiation hESF-DIF medium containing SB-431542 (10 μM) for 10 days. Control cells were treated with solvent only (0.1% DMSO). Expression levels of hepatocyte (C) and cholangiocyte (D) marker genes were measured by real-time RT-PCR. On the *y*-axis, the gene expression level of hepatocyte markers in untreated cells (control) was taken as 1.0. (E) HBC colony formation assay in the presence or absence of 10 ng/ml TGFβ1, TGFβ2 or TGFβ3. HBCs were plated at 200 cells/cm^2 on human LN111-coated dishes. The colonies were separated into four groups based on the expression of ALB and CK19: double-negative, ALB negative and CK19 positive, ALB positive and CK19 negative, and double positive. The numbers represent wells in which the colony was observed in three 96-well plates (total 288 wells). Five days after plating, the cells were fixed with 4% PFA and used for double immunostaining. **P*<0.05, ***P*<0.01 (compared with NONE). Error bars indicate s.d. Statistical analysis was performed using the unpaired two-tailed Student's *t*-test (*n*=3).

c/EBP binding site was found in the *TGFBR2* promoter region (Fig. 4B). A reporter assay of the *TGFBR2* promoter region showed that c/EBPβ activates *TGFBR2* promoter activity, whereas c/EBPα inhibits it (Fig. 4C). In addition, *TGFBR2* expression was downregulated by Ad-c/EBPα transduction, whereas *TGFBR2* was upregulated by Ad-c/EBPβ transduction in HepG2 cells (TGFBR2 positive) (Fig. 4D). We ascertained the expression of *c/EBPα* or *c/EBPβ* (*CEBPA* or *CEBPB* – Human Gene Nomenclature Committee) in the Ad-c/EBPα- or Ad-c/EBPβ-transduced cells, respectively (supplementary material Fig. S4). These results demonstrated that the promoter activity and expression of *TGFBR2* were directly regulated by both c/EBPα and c/EBPβ.

c/EBPs determine the cell fate decision of HBCs via regulation of TGFBR2 expression

To elucidate the relationship between TGFBR2 and c/EBPs (c/EBPα and c/EBPβ) in the hepatoblast fate decision, we first examined the temporal gene expression patterns of *TGFBR2*, *c/EBPα* and *c/EBPβ* in hepatocyte and cholangiocyte differentiation. During hepatocyte differentiation, *TGFBR2* expression was downregulated, whereas *c/EBPα* was upregulated (supplementary material Fig. S7A, top). During cholangiocyte differentiation, *c/EBPα* was downregulated, whereas *TGFBR2* and *c/EBPβ* were upregulated (supplementary material Fig. S7A, bottom). In addition, the ratio of *c/EBPα* to *c/EBPβ* was significantly increased in hepatocyte differentiation, but significantly reduced in cholangiocyte differentiation (supplementary material Fig. S7B). High-level expression of *c/EBPα* was detected in TGFBR2-negative cells, but not in TGFBR2-hi cells (supplementary material Fig. S7C). By contrast, high-level expression of *c/EBPβ* was detected in TGFBR2-hi cells, but not in TGFBR2-negative cells. These results suggest that TGFBR2 is negatively regulated by c/EBPα and positively regulated by c/EBPβ in the differentiation model from HBCs as well as in the HepG2 cell line (Fig. 4).

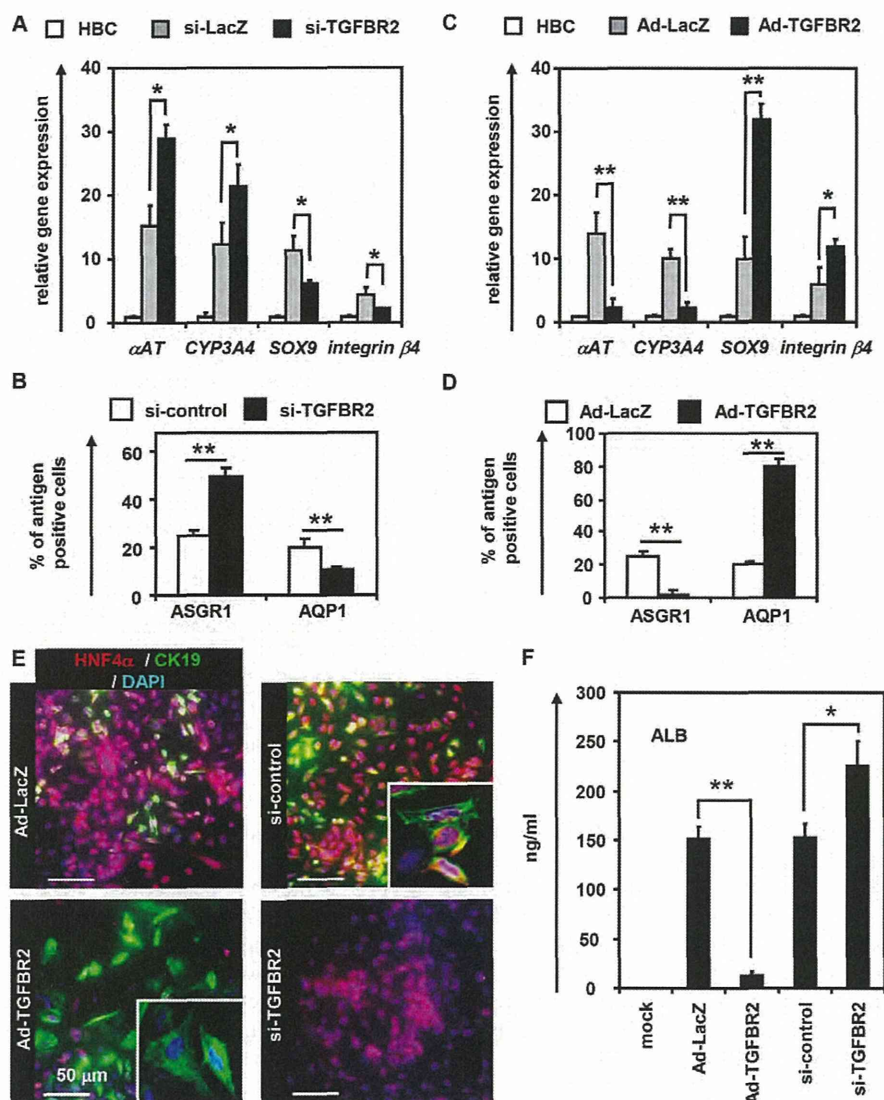

Fig. 3. TGFBR2 regulates bi-directional differentiation of HBCs. (A) HBCs were transfected with 50 nM control siRNA (si-control) or TGFBR2-suppressing siRNA (si-TGFBR2) and cultured in differentiation hESF-DIF medium for 10 days. The expression levels of hepatocyte (*αAT* and *CYP3A4*) or cholangiocyte (*SOX9* and integrin β4) markers were measured by real-time RT-PCR. On the *y*-axis, the gene expression level in HBCs was taken as 1.0. (B) On day 10 after siRNA transfection, the efficiency of hepatocyte or cholangiocyte differentiation was measured by estimating the percentage of ASGR1-positive or AQP1-positive cells, respectively, by FACS analysis. (C) HBCs were transduced with 3000 VPs/cell of Ad-LacZ or Ad-TGFBR2 for 1.5 hours and cultured in differentiation hESF-DIF medium for 10 days. Expression levels of hepatocyte or cholangiocyte marker genes were measured by real-time RT-PCR. On the *y*-axis, gene expression levels in the HBCs was taken as 1.0. (D) On day 10 after Ad vector transduction, the efficiency of hepatocyte or cholangiocyte differentiation was measured by estimating the percentage of ASGR1-positive or AQP1-positive cells, respectively, by FACS analysis. (E,F) The si-control, si-TGFBR2, Ad-LacZ- or Ad-TGFBR2-transfected/transduced HBCs ($1.0{\times}10^6$ cells) were transplanted into CCl_4-treated (2 mg/kg) *Rag2/Il2rg* double-knockout mice by intrasplenic injection. (E) Expression of human HNF4α (red) and CK19 (green) was examined by double immunohistochemistry 2 weeks after transplantation. Nuclei were counterstained with DAPI (blue). (F) Levels of human ALB in recipient mouse serum were measured 2 weeks after transplantation. *$P<0.05$, **$P<0.01$ (compared with Ad-LacZ-transduced or si-control-transfected cells). Error bars indicate s.d. Statistical analysis was performed using the unpaired two-tailed Student's *t*-test ($n=3$).

ChIP experiments showed that c/EBPα or c/EBPβ is recruited to the *TGFBR2* promoter region containing the c/EBP binding site in hepatocyte-like cells or cholangiocyte-like cells, respectively (Fig. 5A), suggesting that c/EBPα and c/EBPβ oppositely regulate *TGFBR2* promoter activity in the differentiation from HBCs. We confirmed that c/EBPα or c/EBPβ was mainly recruited to the *TGFBR2* promoter region containing the c/EBP binding site in TGFBR-negative or TGFBR2-positive cells, respectively (supplementary material Fig. S7D). Taken together, we concluded that c/EBPα and c/EBPβ are able to regulate the cell fate decision of HBCs via regulation of TGFBR2 expression. During differentiation from HBCs, *TGFBR2* expression was negatively regulated by c/EBPα and positively regulated by c/EBPβ (Fig. 5B). To examine whether c/EBPα or c/EBPβ could regulate the differentiation from HBCs, *in vitro* gain- and loss-of-function analyses were performed. si-c/EBPα transfection downregulated hepatocyte marker gene expression, whereas it upregulated cholangiocyte marker genes (Fig. 5C). By contrast, si-c/EBPβ transfection upregulated hepatocyte marker and downregulated cholangiocyte marker gene expression (Fig. 5C). In accordance, Ad-c/EBPα transduction upregulated hepatocyte marker genes and downregulated cholangiocyte markers (Fig. 5D), whereas Ad-c/EBPβ transduction downregulated hepatocyte markers and upregulated cholangiocyte marker genes. Promotion of hepatocyte differentiation by Ad-c/EBPα transduction was inhibited by Ad-TGFBR2 transduction, whereas inhibition of cholangiocyte differentiation by Ad-c/EBPα transduction was rescued by Ad-TGFBR2 transduction (Fig. 5E). In addition, promotion of hepatocyte differentiation by si-c/EBPβ transfection was inhibited by Ad-TGFBR2 transduction, whereas inhibition of cholangiocyte differentiation by si-c/EBPβ transfection was rescued by Ad-TGFBR2 transduction (Fig. 5F). We further confirmed that inhibition of hepatocyte differentiation by si-c/EBPα-transfection was rescued by si-TGFBR2 transfection (supplementary material Fig. S8). Taken together, these results led us to conclude that c/EBPα and c/EBPβ could determine the cell fate of HBCs by negatively and positively regulating TGFBR2 expression, respectively (supplementary material Fig. S9).

c/EBPs organize the differentiation of fetal mouse hepatoblasts through regulation of TGFBR2 expression

We have demonstrated that c/EBPs may determine the HBC fate decision via regulation of the expression level of TGFBR2. To examine whether our findings could be replicated in native liver

Development

Development (2014) doi:10.1242/dev.103168

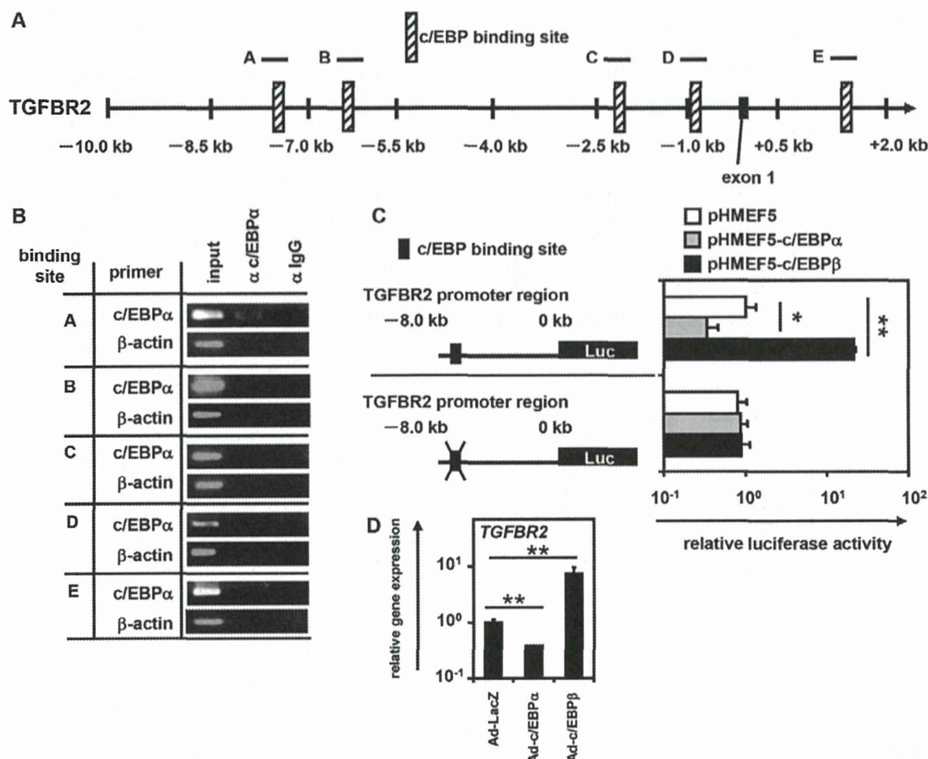

Fig. 4. *TGFBR2* promoter activity and expression are negatively regulated by c/EBPα and positively regulated by c/EBPβ. (A) Candidate c/EBP binding sites (hatched boxes) in the *TGFBR2* promoter region as predicted using rVista 2.0 (see supplementary material Fig. S7). (B) hESCs (H9 cells) were differentiated into hepatoblasts and then a ChIP assay performed. The antibodies and primers employed are summarized in supplementary material Tables S1 and S4. (C) HEK293 cells were transfected with firefly luciferase (Luc) expression plasmids containing the promoter region of *TGFBR2*. In addition, empty plasmid (pHMEF5), c/EBPα expression plasmid (pHMEF5-c/EBPα) or c/EBPβ expression plasmid (pHMEF5-c/EBPβ) was transfected. After 36 hours, a dual luciferase assay was performed. Base pair positions are relative to the translation start site (+1). (D) HepG2 cells (TGFBR2-positive cells) were transduced with 3000 VPs/cell of Ad-LacZ, Ad-c/EBPα or Ad-c/EBPβ for 1.5 hours and cultured for 48 hours. The expression level of *TGFBR2* in HepG2 cells was measured by real-time RT-PCR. On the *y*-axis, the gene expression level in Ad-LacZ-transduced cells was taken as 1.0. *$P<0.05$, **$P<0.01$. Error bars indicate s.d. Statistical analysis was performed using the unpaired two-tailed Student's *t*-test ($n=3$).

development, fetal hepatoblasts were purified from E13.5 mice. The gene expression level of *TGFBR2* in fetal mouse hepatoblasts was negatively or positively regulated by c/EBPα or c/EBPβ, respectively (Fig. 6A,B). The promotion of hepatocyte differentiation by Ad-c/EBPα transduction was inhibited by Ad-TGFBR2 transduction, whereas the inhibition of cholangiocyte differentiation by Ad-c/EBPα transduction was rescued by Ad-TGFBR2 transduction (Fig. 6C). In addition, the promotion of hepatocyte differentiation by si-c/EBPβ transfection was inhibited by Ad-TGFBR2 transduction, whereas the inhibition of cholangiocyte differentiation by si-c/EBPβ transfection was rescued by Ad-TGFBR2 transduction (Fig. 6D). Taken together, these results led us to conclude that c/EBPα and c/EBPβ could determine the cell fate of fetal mouse hepatoblasts by negatively and positively regulating TGFBR2 expression, respectively. Our *in vitro* differentiation system could also prove useful in elucidating the molecular mechanisms of human liver development.

DISCUSSION

The purpose of this study was to better understand the molecular mechanisms of the hepatoblast fate decision in humans. To elucidate the molecular mechanisms of liver development, both conditional knockout mouse models and cell culture systems are useful. For example, DeLaForest et al. demonstrated the role of HNF4α in hepatocyte differentiation using hESC culture systems (DeLaForest et al., 2011). The technology for inducing hepatocyte differentiation from hESCs has recently been dramatically advanced (Takayama et al., 2012a). Because it is possible to generate functional HBCs from hESCs, which can self-replicate and differentiate into both hepatocyte and cholangiocyte lineages (supplementary material Fig. S1 and Fig. 1), the differentiation model of HBCs generated from hESCs should provide a powerful tool for analyzing the molecular mechanisms of human liver development.

In this study, the molecular mechanisms of the hepatoblast fate decision were elucidated using hESC culture systems. HBCs cultured on human LN111 expressed hepatoblast markers (supplementary material Fig. S1) and had the ability to differentiate into both hepatocyte-like cells and cholangiocyte-like cells (Fig. 1). Because a previous study showed that low and high concentrations of TGFβ were required for hepatocyte and cholangiocyte differentiation, respectively (Clotman et al., 2005), we expected that TGFBR2 might contribute to the hepatoblast fate decision. Although TGFβ1, β2 and β3 are all ligands of TGFBR2, TGFβ3 did not promote cholangiocyte differentiation (Fig. 2). This might have been because only TGFβ3 is unable to upregulate the expression of *SOX9*, which is the key factor in bile duct development *in vivo* and cholangiocyte differentiation *in vitro* (Antoniou et al., 2009). We examined the function of TGFBR2 in the hepatoblast fate decision, and found that its overexpression promoted cholangiocyte differentiation, whereas TGFBR2 knockdown promoted hepatocyte differentiation (Fig. 3). Although an exogenous TGFβ ligand was not added to the differentiation medium, the endogenous TGFβ ligand present in Matrigel, which was used in our differentiation protocol, might have bound to TGFBR2. It might also be that the cells committed to the biliary lineage express TGFβ, as a previous study showed that bile duct epithelial cells express TGFβ (Lewindon et al., 2002).

To examine the molecular mechanism regulating TGFBR2 expression, the *TGFBR2* promoter region was analyzed (Fig. 4). *TGFBR2* promoter activity was negatively regulated by c/EBPα and positively regulated by c/EBPβ. c/EBPα overexpression downregulated *TGFBR2* promoter activity in spite of the fact that c/EBPα protein has no repression domain (Yoshida et al., 2006). CTBP1 and CTBP2 (Vernochet et al., 2009) are known to be co-repressors of c/EBPα, and as such constitute candidate co-repressors recruited to the c/EBP binding site in the *TGFBR2* promoter region.

Development (2014) doi:10.1242/dev.103168

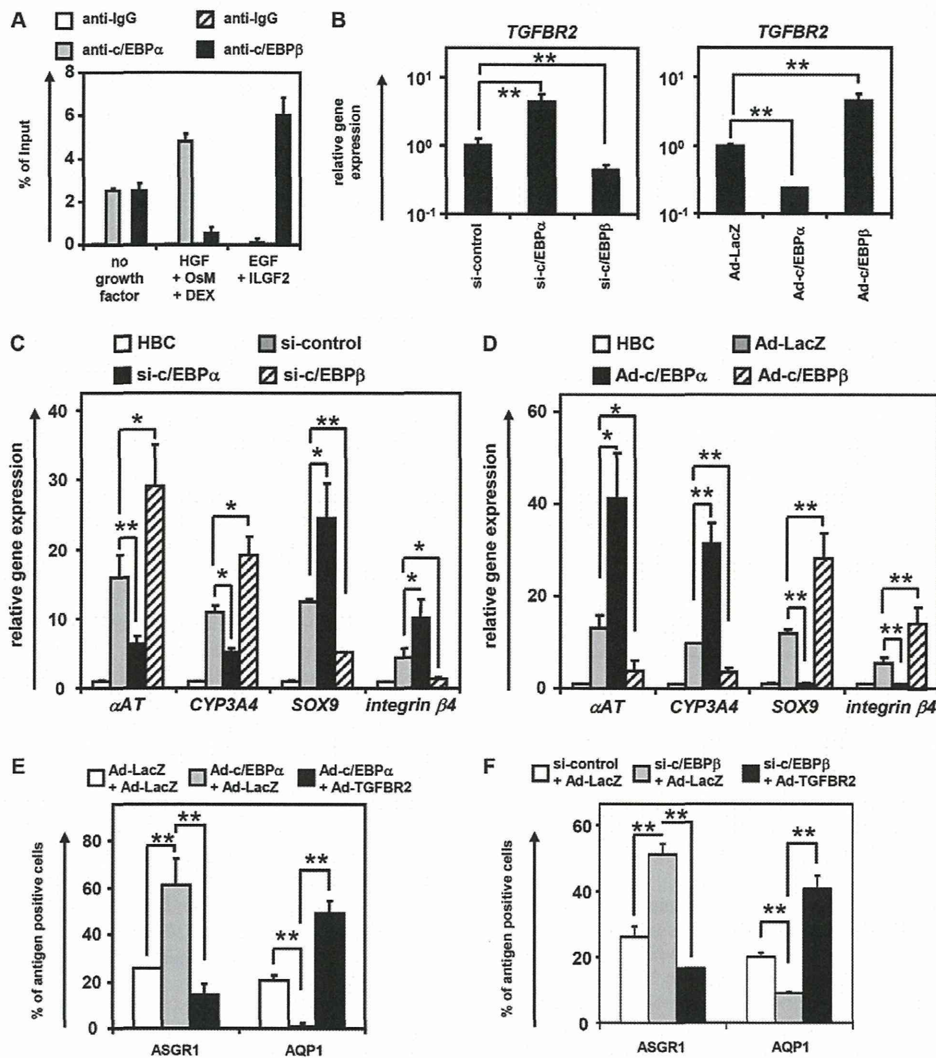

Fig. 5. c/EBPα and c/EBPβ promote hepatocyte and cholangiocyte differentiation by regulating *TGFBR2* expression, respectively. (A) HBCs were differentiated into hepatocyte-like cells or cholangiocyte-like cells according to the scheme outlined in Fig. 1A. On day 10 after hepatocyte or cholangiocyte differentiation, recruitment of c/EBPα or c/EBPβ to the *TGFBR2* promoter region was examined by ChIP assay. (B-D) HBCs were transfected with 50 nM si-control, si-c/EBPα or si-c/EBPβ and cultured in differentiation hESF-DIF medium for 10 days (B left, C). The expression levels of *TGFBR2* and hepatocyte and cholangiocyte markers were then measured by real-time RT-PCR. (B right, D) HBCs were transduced with 3000 VPs/cell of Ad-LacZ, Ad-c/EBPα or Ad-c/EBPβ for 1.5 hours and cultured in differentiation hESF-DIF medium for 10 days. The expression levels of *TGFBR2* and hepatocyte and cholangiocyte markers were then measured by real-time RT-PCR. On the *y*-axis, the gene expression level in the si-control-transfected or Ad-LacZ-transduced cells was taken as 1.0 in B, and levels in HBCs were taken as 1.0 in C and D. (E) HBCs were transduced with 3000 VPs/cell each of Ad-LacZ + Ad-LacZ, Ad-c/EBPα + Ad-LacZ, or Ad-c/EBPα + Ad-TGFBR2 for 1.5 hours and cultured in differentiation hESF-DIF medium for 10 days. The efficiency of hepatocyte or cholangiocyte differentiation was measured by estimating the percentage of ASGR1-positive or AQP1-positive cells, respectively, by FACS analysis. (F) HBCs were transduced with 3000 VPs/cell of Ad-LacZ or Ad-TGFBR2 and then transfected with 50 nM si-control or si-c/EBPβ and cultured in hESF-DIF medium for 10 days. The efficiency of hepatocyte or cholangiocyte differentiation was measured by estimating the percentage of ASGR1-positive or AQP1-positive cells, respectively, by FACS analysis. **P*<0.05, ***P*<0.01. Error bars indicate s.d. Statistical analysis was performed using the unpaired two-tailed Student's *t*-test (*n*=3).

Proteome analysis of c/EBPα would provide an opportunity to identify the co-repressor of c/EBPα. Because large numbers of nearly homogeneous hepatoblasts can be differentiated from hESCs, as compared with the isolation of fetal liver hepatoblasts, hepatocyte differentiation technology from hESCs might prove useful in proteome analysis.

We found that Ad-c/EBPα transduction could promote hepatocyte differentiation by suppressing TGFBR2 expression (Fig. 5). Our findings might thus provide a detailed explanation of the phenotype of *c/EBPα* knockout mice; that is, hepatocyte differentiation is inhibited and cholangiocyte differentiation is promoted in these mice (Yamasaki et al., 2006). We also found that Ad-c/EBPβ transduction could promote cholangiocyte differentiation by enhancing TGFBR2 expression. Because both c/EBPα and c/EBPβ can bind to the same binding site, reciprocal competition for binding is likely to be influenced by regulating c/EBPα or c/EBPβ expression. Therefore, the expression ratio between c/EBPα and c/EBPβ might determine the cell fate of hepatoblasts by regulating the expression level of TGFBR2. We confirmed that our findings could be reproduced in fetal mouse hepatoblasts (Fig. 6). Because a previous study had

Development (2014) doi:10.1242/dev.103168

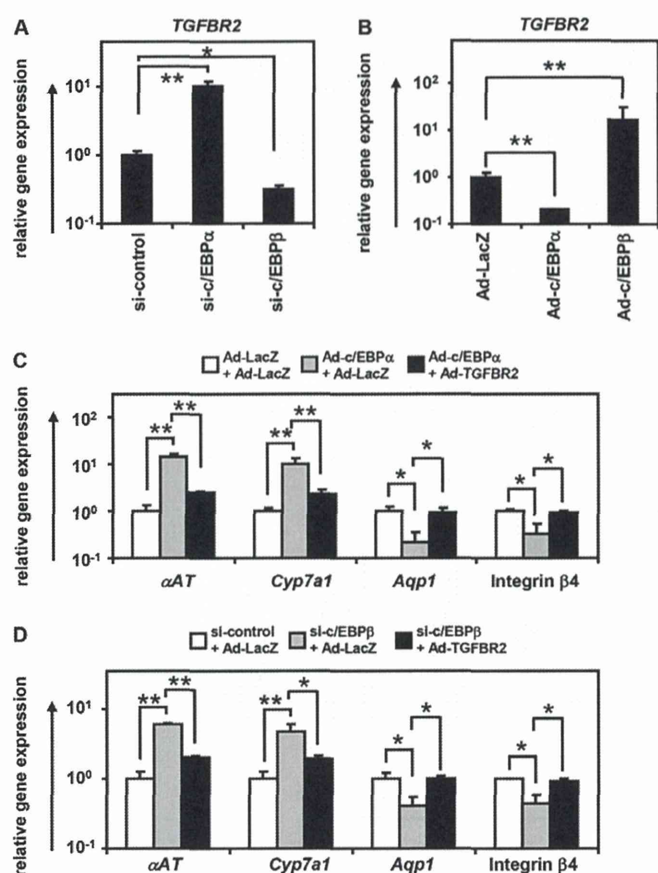

Fig. 6. c/EBPs control the differentiation of fetal mouse hepatoblasts through regulation of TGFBR2 expression. Fetal mouse hepatoblasts (Dlk1-positive cells; the purity was over 98%) were sorted from E13.5 mouse liver. (A) Fetal mouse hepatoblasts were transfected with 50 nM si-control, si-c/EBPα or si-c/EBPβ and cultured for 5 days. The expression of *TGFBR2* was measured by real-time RT-PCR. (B) Fetal mouse hepatoblasts were transduced with 3000 VPs/cell of Ad-LacZ, Ad-c/EBPα or Ad-c/EBPβ for 1.5 hours and cultured for 5 days. The expression of *TGFBR2* was measured by real-time RT-PCR. On the *y*-axis, the gene expression level in the si-control-transfected cells or Ad-LacZ-transduced cells was taken as 1.0. (C) Fetal mouse hepatoblasts were transduced with 3000 VPs/cell each of Ad-LacZ + Ad-LacZ, Ad-c/EBPα + Ad-LacZ, or Ad-c/EBPα + Ad-TGFBR2 for 1.5 hours and cultured for 5 days. On day 5, the expression levels of hepatocyte (*αAT* and *Cyp7a1*) and cholangiocyte (*Aqp1* and integrin β4) markers were measured by real-time RT-PCR. (D) Fetal mouse hepatoblasts were transduced with 3000 VPs/cell of Ad-LacZ or Ad-TGFBR2 and then transfected with 50 nM si-control or si-c/EBPβ and cultured for 5 days. On day 5, the gene levels of hepatocyte (*αAT* and *Cyp7a1*) and cholangiocyte (*Aqp1* and integrin β4) markers were measured by real-time RT-PCR. On the *y*-axis, the gene expression level in the si-control-transfected or Ad-LacZ-transduced cells was taken as 1.0. $^{*}P<0.05$, $^{**}P<0.01$. Error bars indicate s.d. Statistical analysis was performed using the unpaired two-tailed Student's *t*-test ($n=3$).

shown that the addition of hepatocyte growth factor (HGF) to hepatoblasts upregulated the expression of c/EBPα and downregulated the expression of c/EBPβ (Suzuki et al., 2003), the ratio between c/EBPα and c/EBPβ might be determined by HGF during hepatocyte differentiation.

In this study, we have identified for the first time that *TGFBR2* is a target of c/EBPs in the hepatoblast fate decision (supplementary material Fig. S9). c/EBPα promotes hepatocyte differentiation by downregulating the expression of TGFBR2, whereas c/EBPβ promotes cholangiocyte differentiation by upregulating TGFBR2 expression. This study might have revealed a molecular mechanism underlying the lineage commitment of human hepatoblasts controlled by a gradient of TGFβ signaling. We believe that similar procedures that adopt the model of human pluripotent stem cell (including human iPS cell) differentiation will be used not only for the elucidation of molecular mechanisms underlying human hepatocyte and biliary differentiation but also for investigating the causes of congenital anomalies of the human liver and biliary tract.

MATERIALS AND METHODS

Ad vectors

Ad vectors were constructed by an improved *in vitro* ligation method (Mizuguchi and Kay, 1998; Mizuguchi and Kay, 1999). The human *c/EBPα* and *c/EBPβ* genes (accession numbers NM_004364 and NM_005194, respectively) were amplified by PCR using the following primers: c/EBPα, Fwd 5′-GCTCTAGATGCCGGGAGAACTCTAACTC-3′ and Rev 5′-GCGGTACCAAACCACTCCCTGGGTCC-3′; c/EBPβ, Fwd 5′-GCATCTAGATTCATGCAACGCCTGGTG-3′ and Rev 5′-ATAGGTACCTAAAATTACCGACGGGCTCC-3′. The human *TGFBR2* gene was purchased from Addgene (plasmid 16622). The human *c/EBPα*, *c/EBPβ* or *TGFBR2* gene was inserted into pBSKII (Invitrogen), resulting in pBSKII-c/EBPα, -c/EBPβ or -TGFBR2. Then, human *c/EBPα*, *c/EBPβ* or *TGFBR2* was inserted into pHMEF5 (Kawabata et al., 2005), which contains the human elongation factor 1α (*EF1α*, also known as *EEF1A1*) promoter, resulting in pHMEF5-c/EBPα, -c/EBPβ or -TGFBR2. pHMEF5-c/EBPα, -c/EBPβ or -TGFBR2 was digested with I-*Ceu*I/PI-*Sce*I and ligated into I-*Ceu*I/PI-*Sce*I-digested pAdHM41-K7 (Koizumi et al., 2003), resulting in pAd-c/EBPα, -c/EBPβ or -TGFBR2. The human *EF1α* promoter-driven *lacZ*- or FOXA2-expressing Ad vectors (Ad-LacZ or Ad-FOXA2, respectively) were constructed previously (Takayama et al., 2012b; Tashiro et al., 2008). All Ad vectors contain a stretch of lysine residues (K7) in the C-terminal region of the fiber knob for more efficient transduction of hESCs, definitive endoderm cells and HBCs, in which transfection efficiency was almost 100%, and the Ad vectors were purified as described previously (Takayama et al., 2012a; Takayama et al., 2011). The vector particle (VP) titer was determined by a spectrophotometric method (Maizel et al., 1968).

hESC culture

The H9 hESC line (WiCell Research Institute) was maintained on a feeder layer of mitomycin C-treated mouse embryonic fibroblasts (Merck Millipore) in ReproStem medium (ReproCELL) supplemented with 5 ng/ml FGF2 (Katayama Kagaku Kogyo). H9 was used following the Guidelines for Derivation and Utilization of Human Embryonic Stem Cells of the Ministry of Education, Culture, Sports, Science and Technology of Japan and the study was approved by the Independent Ethics Committee.

Generation and maintenance of hESC-derived HBCs

Before the initiation of cellular differentiation, the hESC medium was exchanged for a defined serum-free medium, hESF9, and cultured as previously reported (Furue et al., 2008). The differentiation protocol for the induction of definitive endoderm cells and HBCs was based on our previous reports with some modifications (Takayama et al., 2012a; Takayama et al., 2012b; Takayama et al., 2011). Briefly, in mesendoderm differentiation, hESCs were cultured for 2 days on Matrigel Matrix (BD Biosciences) in differentiation hESF-DIF medium, which contains 100 ng/ml activin A (R&D Systems); hESF-DIF medium was purchased from Cell Science & Technology Institute; differentiation hESF-DIF medium was supplemented with 10 μg/ml human recombinant insulin, 5 μg/ml human apotransferrin, 10 μM 2-mercaptoethanol, 10 μM ethanolamine, 10 μM sodium selenite, 0.5 mg/ml bovine fatty acid-free serum albumin (all from Sigma) and 1×B27 Supplement (without vitamin A; Invitrogen). To generate definitive endoderm cells, the mesendoderm cells were transduced with 3000 VPs/cell of FOXA2-expressing Ad vector (Ad-FOXA2) for 1.5 hours on day 2 and cultured until day 6 on Matrigel in differentiation hESF-DIF medium supplemented with 100 ng/ml activin A. For induction of the HBCs, the

definitive endoderm cells were cultured for 3 days on Matrigel in differentiation hESF-DIF medium supplemented with 20 ng/ml BMP4 (R&D Systems) and 20 ng/ml FGF4 (R&D Systems). Transient overexpression of FOXA2 in the mesendoderm cells is not necessary for establishing HBCs, but it is helpful for efficient generation of the HBCs. The HBCs were first purified from the hESC-derived cells (day 9) by selecting attached cells on a human recombinant LN111 (BioLamina)-coated dish 15 minutes after plating (Takayama et al., 2013). The HBCs were cultured on a human LN111-coated dish (2.0×10^4 cells/cm^2) in maintenance DMEM/F12 medium [DMEM/F12 medium (Invitrogen) supplemented with 10% fetal bovine serum (FBS), 1× insulin/transferrin/selenium, 10 mM nicotinamide, 0.1 µM dexamethasone (DEX) (Sigma), 20 mM HEPES, 25 mM $NaHCO_3$, 2 mM L-glutamine, and penicillin/streptomycin] which contained 40 ng/ml HGF (R&D Systems) and 20 ng/ml epidermal growth factors (EGF) (R&D Systems). The medium was refreshed every day. The HBCs were dissociated with Accutase (Millipore) into single cells, and subcultured every 6 or 7 days. The HBCs used in this study were passaged more than three times.

In vitro hepatocyte and cholangiocyte differentiation

To induce hepatocyte differentiation, the HBCs were cultured on a Matrigel-coated dish (7.5×10^4 cells/cm^2) in Hepatocyte Culture Medium (HCM without EGF; Lonza) supplemented with 20 ng/ml HGF, 20 ng/ml Oncostatin M (OsM) (R&D Systems) and 1 µM DEX. To induce cholangiocyte differentiation, the HBCs were cultured in collagen gel. To establish collagen gel plates, 500 µl collagen gel solution [400 µl type I-A collagen (Nitta gelatin), 50 µl 10× DMEM and 50 µl 200 mM HEPES buffer containing 2.2% $NaHCO_3$ and 0.05 M NaOH] was added to each well, and then the plates were incubated at 37°C for 30 minutes. The HBCs (5×10^4 cells) were resuspended in 500 µl differentiation DMEM/F12 medium [DMEM/F12 medium supplemented with 20 mM HEPES, 2 mM L-glutamine, 100 ng/ml EGF and 40 ng/ml ILGF2 (IGF2)], and then mixed with 500 µl of the collagen gel solution and plated onto the basal layer of collagen. After 30 minutes, 2 ml differentiation DMEM/F12 medium was added to the well.

Inhibition of TGFβ signaling

SB-431542 (Santa Cruz Biotechnology), which is a small molecule that acts as a selective inhibitor of activin receptor-like kinase (ALK) receptors [ALK4, ALK5 and ALK7 (also known as ACVR1B, TGFBR1 and ACVR1C)], was used to inhibit TGFβ signaling in HBCs.

Flow cytometry

Single-cell suspensions of hESC-derived cells were fixed with 2% paraformaldehyde (PFA) at 4°C for 20 minutes, and then incubated with primary antibody (supplementary material Table S1) followed by secondary antibody (supplementary material Table S2). Flow cytometry analysis was performed using a FACS LSR Fortessa flow cytometer (BD Biosciences). Cell sorting was performed using a FACS Aria (BD Biosciences).

RNA isolation and reverse transcription (RT)-PCR

Total RNA was isolated from hESCs and their derivatives using ISOGENE (Nippon Gene). cDNA was synthesized using 500 ng total RNA with the SuperScript VILO cDNA Synthesis Kit (Invitrogen). Real-time RT-PCR was performed with SYBR Green PCR Master Mix (Applied Biosystems) using an Applied Biosystems StemOnePlus real-time PCR system. Relative quantification was performed against a standard curve and the values were normalized against the input determined for the housekeeping gene *GAPDH*. Primers are described in supplementary material Table S3.

Immunohistochemistry

Cells were fixed with 4% PFA. After incubation with 0.1% Triton X-100 (Wako), blocking with Blocking One (Nakalai Tesque) or PBS containing 2% FBS, 2% BSA and 0.1% Triton X-100, the cells were incubated with primary antibody (supplementary material Table S1) at 4°C overnight, followed by secondary antibody (supplementary material Table S2) at room temperature for 1 hour. Immunopositive cells were counted in at least eight randomly chosen fields.

HBC colony formation assay

For the colony formation assay, HBCs were cultured at a low density (200 cells/cm^2) on a human LN111-coated dish in maintenance DMEM/F12 medium supplemented with 25 µM LY-27632 (ROCK inhibitor; Millipore).

Transplantation of clonally derived HBCs

Clonally derived HBCs were dissociated using Accutase and then suspended in maintenance DMEM/F12 medium without serum. The HBCs (1×10^6 cells) were transplanted 24 hours after administration of CCl_4 (2 mg/kg) by intrasplenic injection into 8- to 10-week-old *Rag2/Il2rg* double-knockout mice. Recipient mouse livers and blood were harvested 2 weeks after transplantation. Grafts were fixed with 4% PFA and processed for immunohistochemistry. Serum was extracted and subjected to ELISA. All animal experiments were conducted in accordance with institutional guidelines.

ELISA

Levels of human ALB in mouse serum were examined by ELISA using kits from Bethyl Laboratories according to the manufacturer's instructions.

Culture of mouse Dlk1$^+$ cells

Dlk1$^+$ hepatoblasts were isolated from E13.5 mouse livers using anti-mouse Dlk1 monoclonal antibody (MBL International Corporation, D187-4) as described previously (Tanimizu et al., 2003). Dlk1$^+$ cells were resuspended in DMEM/F12 (Sigma) containing 10% FBS, 1× insulin/transferrin/selenium (ITS), 10 mM nicotinamide (Wako), 0.1 µM DEX and 5 mM L-glutamine. Cells were plated on laminin-coated dishes and cultured in medium containing 20 ng/ml HGF, EGF and 25 µM LY-27632 (ROCK inhibitor).

lacZ assay

Hepatoblasts were transduced with Ad-LacZ at 3000 VPs/cell for 1.5 hours. The day after transduction (day 10), 5-bromo-4-chloro-3-indolyl β-D-galactopyranoside (X-Gal) staining was performed as described previously (Kawabata et al., 2005).

Reporter assays

The effects of c/EBPα or c/EBPβ overexpression on *TGFBR2* promoter activity were examined using a reporter assay. An 8 kb fragment of the 5′ flanking region of the *TGFBR2* gene was amplified by PCR using the following primers: Fwd, 5′-CCGAGCTCATGTTTGATGAAGTGTCTAG-CTTCCAAGG-3′; Rev, 5′-GGCTCGAGCCTCGACGTCCAGCCCCT-3′. The fragment was inserted into the *SacI*/*XhoI* sites of pGL3-basic (Promega), resulting in a pGL3-*TGFBR2* promoter region (pGL3-TGFBR2-PR). To generate a *TGFBR2* promoter region containing mutations in the c/EBP binding site, the following primers were used in PCR (mutations are indicated by lowercase letters): Fwd, 5′-CACTAGTATTCAgTG-AtCcgAAAATATGG-3′; Rev, 5′-CACTAGTATTCAgTGAtCcgAAAA-TATGG-3′; this resulted in pGL3-mTGFBR2-PR. HEK293 cells were maintained in DMEM (Wako) supplemented with 10% FBS, penicillin and streptomycin, and 2 mM L-glutamine. In reporter assays, 60 ng pGL3-TGFBR2-PR or pGL3-mTGFBR2-PR was transfected together with 720 ng each expression plasmid (pHMEF5, pHMEF5-c/EBPα and pHMEF5-c/EBPβ) and 60 ng internal control plasmid (pCMV-Renilla luciferase) using Lipofectamine 2000 reagent (Invitrogen). Transfected cells were cultured for 36 hours, and a Dual Luciferase Assay (Promega) was performed according to the manufacturer's instructions.

siRNA-mediated knockdown

Predesigned siRNAs targeting *c/EBPα*, *c/EBPβ* and *TGFBR2* mRNAs were purchased from Thermo Scientific Dharmacon. Cells were transfected with 50 nM siRNA using RNAiMAX (Invitrogen) transfection reagent according to the manufacturer's instructions. As a negative control, we used scrambled siRNA (Qiagen) of a sequence showing no significant similarity to any mammalian gene.

Chromatin immunoprecipitation (ChIP) assay

The ChIP assay kit was purchased from Upstate. Cells were crosslinked using formaldehyde at a final concentration of 1% at 37°C for 10 minutes, and then genomic DNA was fragmented by sonicator. The resulting DNA-protein complexes were immunoprecipitated using the antibodies described in supplementary material Table S1 or control IgG as described in supplementary material Table S2. The precipitated DNA fragments were analyzed by real-time RT-PCR using the primers shown in supplementary material Table S4 to amplify the *TGFBR2* promoter region including the c/EBP binding sites or β-actin locus as a control. The results of quantitative ChIP analysis (Fig. 5A) were expressed as the amount of amplified *TGFBR2* promoter region relative to input DNA taken as 100%.

Statistical analysis

Statistical analysis was performed using an unpaired two-tailed Student's t-test. All data are represented as mean ± s.d. (n=3).

Acknowledgements

We thank Natsumi Mimura, Yasuko Hagihara and Hiroko Matsumura for excellent technical support.

Competing interests

The authors declare no competing financial interests.

Author contributions

K. Takayama, K.K. and H.M. developed the concepts or approach; K. Takayama, Y.N., K.O., H.O. and T.Y. performed experiments; K. Takayama, K.K., M.I., K. Tashiro, F.S., T.H., T.O., M.F.K. and H.M. performed data analysis; K. Takayama, K.K. and H.M. prepared or edited the manuscript prior to submission.

Funding

H.M., K.K., M.K.F. and T.H. were supported by grants from the Ministry of Health, Labor, and Welfare of Japan (MEXT). H.M. was also supported by Japan Research Foundation for Clinical Pharmacology, The Uehara Memorial Foundation. K.O. was supported by Special Coordination Funds for Promoting Science and Technology from MEXT. F.S. was supported by Program for Promotion of Fundamental Studies in Health Sciences of the National Institute of Biomedical Innovation (NIBIO). K. Takayama and Y.N. are Research Fellows of the Japan Society for the Promotion of Science.

Supplementary material

Supplementary material available online at
http://dev.biologists.org/lookup/suppl/doi:10.1242/dev.103168/-/DC1

References

Agarwal, S., Holton, K. L. and Lanza, R. (2008). Efficient differentiation of functional hepatocytes from human embryonic stem cells. *Stem Cells* **26**, 1117-1127.

Antoniou, A., Raynaud, P., Cordi, S., Zong, Y., Tronche, F., Stanger, B. Z., Jacquemin, P., Pierreux, C. E., Clotman, F. and Lemaigre, F. P. (2009). Intrahepatic bile ducts develop according to a new mode of tubulogenesis regulated by the transcription factor SOX9. *Gastroenterology* **136**, 2325-2333.

Chen, S. S., Chen, J. F., Johnson, P. F., Muppala, V. and Lee, Y. H. (2000). C/EBPbeta, when expressed from the C/ebpalpha gene locus, can functionally replace C/EBPalpha in liver but not in adipose tissue. *Mol. Cell. Biol.* **20**, 7292-7299.

Clotman, F., Jacquemin, P., Plumb-Rudewiez, N., Pierreux, C. E., Van der Smissen, P., Dietz, H. C., Courtoy, P. J., Rousseau, G. G. and Lemaigre, F. P. (2005). Control of liver cell fate decision by a gradient of TGF beta signaling modulated by Onecut transcription factors. *Genes Dev.* **19**, 1849-1854.

DeLaForest, A., Nagaoka, M., Si-Tayeb, K., Noto, F. K., Konopka, G., Battle, M. A. and Duncan, S. A. (2011). HNF4A is essential for specification of hepatic progenitors from human pluripotent stem cells. *Development* **138**, 4143-4153.

Furue, M. K., Na, J., Jackson, J. P., Okamoto, T., Jones, M., Baker, D., Hata, R., Moore, H. D., Sato, J. D. and Andrews, P. W. (2008). Heparin promotes the growth of human embryonic stem cells in a defined serum-free medium. *Proc. Natl. Acad. Sci. USA* **105**, 13409-13414.

Hansen, A. J., Lee, Y. H., Sterneck, E., Gonzalez, F. J. and Mackenzie, P. I. (1998). C/EBPalpha is a regulator of the UDP glucuronosyltransferase UGT2B1 gene. *Mol. Pharmacol.* **53**, 1027-1033.

Kawabata, K., Sakurai, F., Yamaguchi, T., Hayakawa, T. and Mizuguchi, H. (2005). Efficient gene transfer into mouse embryonic stem cells with adenovirus vectors. *Mol. Ther.* **12**, 547-554.

Kitisin, K., Saha, T., Blake, T., Golestaneh, N., Deng, M., Kim, C., Tang, Y., Shetty, K., Mishra, B. and Mishra, L. (2007). Tgf-Beta signaling in development. *Sci. STKE* **2007**, cm1.

Koizumi, N., Mizuguchi, H., Utoguchi, N., Watanabe, Y. and Hayakawa, T. (2003). Generation of fiber-modified adenovirus vectors containing heterologous peptides in both the HI loop and C terminus of the fiber knob. *J. Gene Med.* **5**, 267-276.

Lewindon, P. J., Pereira, T. N., Hoskins, A. C., Bridle, K. R., Williamson, R. M., Shepherd, R. W. and Ramm, G. A. (2002). The role of hepatic stellate cells and transforming growth factor-beta(1) in cystic fibrosis liver disease. *Am. J. Pathol.* **160**, 1705-1715.

Maizel, J. V., Jr, White, D. O. and Scharff, M. D. (1968). The polypeptides of adenovirus. I. Evidence for multiple protein components in the virion and a comparison of types 2, 7A, and 12. *Virology* **36**, 115-125.

Mizuguchi, H. and Kay, M. A. (1998). Efficient construction of a recombinant adenovirus vector by an improved in vitro ligation method. *Hum. Gene Ther.* **9**, 2577-2583.

Mizuguchi, H. and Kay, M. A. (1999). A simple method for constructing E1- and E1/E4-deleted recombinant adenoviral vectors. *Hum. Gene Ther.* **10**, 2013-2017.

Oe, S., Lemmer, E. R., Conner, E. A., Factor, V. M., Levéen, P., Larsson, J., Karlsson, S. and Thorgeirsson, S. S. (2004). Intact signaling by transforming growth factor beta is not required for termination of liver regeneration in mice. *Hepatology* **40**, 1098-1105.

Plumb-Rudewiez, N., Clotman, F., Strick-Marchand, H., Pierreux, C. E., Weiss, M. C., Rousseau, G. G. and Lemaigre, F. P. (2004). Transcription factor HNF-6/OC-1 inhibits the stimulation of the HNF-3alpha/Foxa1 gene by TGF-beta in mouse liver. *Hepatology* **40**, 1266-1274.

Schmelzer, E., Zhang, L., Bruce, A., Wauthier, E., Ludlow, J., Yao, H. L., Moss, N., Melhem, A., McClelland, R., Turner, W. et al. (2007). Human hepatic stem cells from fetal and postnatal donors. *J. Exp. Med.* **204**, 1973-1987.

Suzuki, A., Iwama, A., Miyashita, H., Nakauchi, H. and Taniguchi, H. (2003). Role for growth factors and extracellular matrix in controlling differentiation of prospectively isolated hepatic stem cells. *Development* **130**, 2513-2524.

Takayama, K., Inamura, M., Kawabata, K., Tashiro, K., Katayama, K., Sakurai, F., Hayakawa, T., Furue, M. K. and Mizuguchi, H. (2011). Efficient and directive generation of two distinct endoderm lineages from human ESCs and iPSCs by differentiation stage-specific SOX17 transduction. *PLoS ONE* **6**, e21780.

Takayama, K., Inamura, M., Kawabata, K., Katayama, K., Higuchi, M., Tashiro, K., Nonaka, A., Sakurai, F., Hayakawa, T., Furue, M. K. et al. (2012a). Efficient generation of functional hepatocytes from human embryonic stem cells and induced pluripotent stem cells by HNF4α transduction. *Mol. Ther.* **20**, 127-137.

Takayama, K., Inamura, M., Kawabata, K., Sugawara, M., Kikuchi, K., Higuchi, M., Nagamoto, Y., Watanabe, H., Tashiro, K., Sakurai, F. et al. (2012b). Generation of metabolically functioning hepatocytes from human pluripotent stem cells by FOXA2 and HNF1α transduction. *J. Hepatol.* **57**, 628-636.

Takayama, K., Nagamoto, Y., Mimura, N., Tashiro, K., Sakurai, F., Tachibana, M., Hayakawa, T., Kawabata, K. and Mizuguchi, H. (2013). Long-term self-renewal of human ES/iPS-derived hepatoblast-like cells on human laminin 111-coated dishes. *Stem Cell Reports* **1**, 322-335.

Tanimizu, N., Nishikawa, M., Saito, H., Tsujimura, T. and Miyajima, A. (2003). Isolation of hepatoblasts based on the expression of Dlk/Pref-1. *J. Cell Sci.* **116**, 1775-1786.

Tashiro, K., Kawabata, K., Sakurai, H., Kurachi, S., Sakurai, F., Yamanishi, K. and Mizuguchi, H. (2008). Efficient adenovirus vector-mediated PPAR gamma gene transfer into mouse embryoid bodies promotes adipocyte differentiation. *J. Gene Med.* **10**, 498-507.

Tomizawa, M., Garfield, S., Factor, V. and Xanthopoulos, K. G. (1998). Hepatocytes deficient in CCAAT/enhancer binding protein alpha (C/EBP alpha) exhibit both hepatocyte and biliary epithelial cell character. *Biochem. Biophys. Res. Commun.* **249**, 1-5.

Vernochet, C., Peres, S. B., Davis, K. E., McDonald, M. E., Qiang, L., Wang, H., Scherer, P. E. and Farmer, S. R. (2009). C/EBPalpha and the corepressors CtBP1 and CtBP2 regulate repression of select visceral white adipose genes during induction of the brown phenotype in white adipocytes by peroxisome proliferator-activated receptor gamma agonists. *Mol. Cell. Biol.* **29**, 4714-4728.

Yamasaki, H., Sada, A., Iwata, T., Niwa, T., Tomizawa, M., Xanthopoulos, K. G., Koike, T. and Shiojiri, N. (2006). Suppression of C/EBPalpha expression in periportal hepatoblasts may stimulate biliary cell differentiation through increased Hnf6 and Hnf1b expression. *Development* **133**, 4233-4243.

Yoshida, Y., Hughes, D. E., Rausa, F. M., III, Kim, I. M., Tan, Y., Darlington, G. J. and Costa, R. H. (2006). C/EBPalpha and HNF6 protein complex formation stimulates HNF6-dependent transcription by CBP coactivator recruitment in HepG2 cells. *Hepatology* **43**, 276-286.

Copyright © 2015 Cognizant Communication Corporation

DOI: 10.3727/096368914X685799

CT-1353 Accepted 12/20/2014 for publication in "Cell Transplantation"

Functional and Electrical Integration of Induced Pluripotent Stem Cell-Derived Cardiomyocytes in a Myocardial Infarction Rat Heart

Short title: Integration of iPSC-cardiomyocytes in the heart

Takahiro Higuchi[1], MD, Shigeru Miyagawa MD, PhD[1], James T. Pearson, PhD[2,3], Satsuki Fukushima MD, PhD[1], Atsuhiro Saito PhD[4], Hirotsugu Tsuchimochi, PhD[5], Takashi Sonobe, PhD[4], Yutaka Fujii, MS[5], Naoto Yagi, PhD[6], Alberto Astolfo, PhD[2], Mikiyasu Shirai, MD PhD[5], Yoshiki Sawa MD, PhD[1]

CELL TRANSPLANTATION The Regenerative Medicine Journal

[1]Department of Cardiac Surgery, Osaka University Graduate School of Medicine, Osaka, Japan, [2]The Australian Synchrotron, Clayton, Victoria Australia, [3]Monash Biomedical Imaging Facility, Monash University, Clayton, Victoria, Australia, [4]Medical Center for Translational Research, Osaka University Hospital, Osaka, Japan, [5]Department of Cardiac Physiology, National Cerebral and Cardiovascular Center Research Institute, Suita, Osaka, Japan, [6]SPring-8/JASRI, Sayo, Hyogo, Japan

Address for Correspondence; Professor Yoshiki Sawa

Department of Cardiovascular Surgery, Osaka University Graduate School of Medicine

2-2 Yamadaoka, Suita, 565-0871 Japan

Telephone; +81668793154, Facsimile; +81668793163

E-mail; sawa-p@surg1.med.osaka-u.ac.jp

Total word count: 5,328 words

CT-1353 Cell Transplantation Early Epub; provisional acceptance 12/04/2014

Copyright © 2015 Cognizant Communication Corporation

ABSTRACT

Functional and Electrical Integration of Induced Pluripotent Stem Cell-Derived Cardiomyocytes in a Myocardial Infarction Rat Heart

Higuchi T, Miyagawa S, Pearson JT, Fukushima S, Saito A, Tsuchimochi H, Sonobe T, Fujii Y,

In vitro expanded beating cardiac myocytes derived from induced pluripotent stem cells (iPSC-CMs) are a promising source of therapy for cardiac regeneration. Meanwhile, the cell-sheet method has been shown to potentially maximize survival, functionality and integration of the transplanted cells into the heart. It is thus hypothesized that transplanted iPSC-CMs in a cell-sheet manner may contribute to functional recovery *via* direct mechanical effects on the myocardial infarction (MI) heart.

: F344/NJcl-rnu/rnu rat were left coronary artery-ligated (n=30), followed by transplantation of Dsred-labeled iPSC-CMs cell-sheets of murine origin over the infarct heart surface. Effects of the treatment were assessed, including *in vivo* molecular/cellular evaluations using a synchrotron radiation scattering technique. Ejection fraction and activation recovery interval were significantly greater from day 3 onwards after iPSC-CMs transplantation compared to those after sham operation. A number of transplanted iPSC-CMs were present on the heart surface expressing cardiac myosin or connexin43 over two weeks, assessed by immunoconfocal microscopy, while mitochondria in the transplanted iPSC-CMs gradually showed mature structure as assessed by electronmicroscopy. Of note, X-ray diffraction identified 1,0 and 1,1 equatorial reflections attributable to myosin and actin-myosin lattice planes typical of organized cardiac muscle fibers within the transplanted cell-sheets at 4 weeks, suggesting cyclic systolic myosin mass transfer to actin filaments in the transplanted iPSC-CMs.

Transplantation of iPSC-CM cell-sheets into the heart yielded functional and electrical recovery with cyclic contraction of transplanted cells in the rat MI heart, indicating that this strategy may be a promising “cardiac muscle replacement” therapy.

Keywords: iPS cell; regeneration therapy; cell-sheet; synchrotron imaging

CELL TRANSPLANTATION The Regenerative Medicine Journal

CT-1353 Cell Transplantation Early Epub; provisional acceptance 12/04/2014

Copyright © 2015 Cognizant Communication Corporation

INTRODUCTION

To increase the number of functional cardiomyocytes in the heart is a goal of regenerative therapy for advanced cardiac failure (14). It has been shown that induced pluripotent stem cells (iPSCs) differentiate into functional cardiomyocytes *in vitro* by specific culture regimens, suggesting that replacement of damaged cardiac tissue might be achieved by transplantation of iPSCs-derived cardiomyocytes (iPSC-CMs) into the damaged area using an appropriate cell-delivery method. Further, it has been shown that the cell-sheet method, in which a scaffold-free sheet-shaped cultured cell-cluster is placed on the surface of the heart, delivers a large number of the cells while preserving the functionality of the cells and the myocardium, indicating that the cell-sheet method may be an ideal delivery method of iPSC-CM to replace the damaged cardiac area (8,9,15). In fact, we reported that transplantation of iPSC-CMs into the heart by the cell-sheet method improves functional performance of the infarcted heart in pigs (5). However, in that study (5), synchronous contraction of the transplanted iPSC-CMs as "cardiac myocytes" that express the regular, cyclic actin-myosin cross-bridge motion, which is the aim of this treatment, was not demonstrated due to the limitations of current image analysis methods *in vivo*.

Shiba et al. reported that the fluorescent signal of calcium sensor, GCaMP3, which has been genetically encoded in the cells prior to transplantation into the heart, was useful for visualizing spontaneous contraction of the transplanted cells in the heart *in vivo* (16). However, the calcium sensor signal does not necessarily correlate with normal cyclic actin-myosin cross-bridge motion. On the other hand, third generation synchrotron radiation (SPring-8, Hyogo, Japan) has been utilized to quantify actin-myosin cross-bridge dynamics in cardiac fibres of localized regions *in vivo* (12,17). We herein hypothesized that transplanted iPSC-CMs in a cell-sheet manner may contribute to functional recovery *via* direct mechanical

CELL TRANSPLANTATION The Regenerative Medicine Journal